Spin-dependent Bohm trajectories associated with an electronic transition in hydrogen

2003 J. Phys. A: Math. Gen. 36 4689

(http://iopscience.iop.org/0305-4470/36/16/317)

INSTITUTE OF PHYSICS PUBLISHING JOURNAL OF PHYSICS A: MATHEMATICAL AND GENERAL

J. Phys. A: Math. Gen. **36** (2003) 4689–4702 PII: S0305-4470(03)52599-9

Spin-dependent Bohm trajectories associated with an electronic transition in hydrogen

C Colijn and E R Vrscay

Department of Applied Mathematics, University of Waterloo, Waterloo, Ontario, Canada N2L 3G1

Received 21 August 2002, in final form 25 February 2003
Published 8 April 2003
Online at stacks.iop.org/JPhysA/36/4689

Abstract

The de Broglie–Bohm causal theory of quantum mechanics with spin-dependence is used to determine electron trajectories when a hydrogen atom is subjected to (semiclassical) radiation. The transition between the 1s ground state and the $2p_0$ state is examined. It is found that transitions can be identified along Bohm trajectories. The trajectories lie on invariant hyperboloid surfaces of revolution in $\mathbf{R}^3$. The energy along the trajectories is also discussed in relation to the hydrogen energy eigenvalues.

PACS number: 03.65.Bz

1. Introduction

In the de Broglie–Bohm causal interpretation of quantum mechanics [1–3], as opposed to the standard 'Copenhagen' interpretation, particles are endowed with well-defined trajectories $\mathbf{x}_i(t)$ that are determined by the wavefunction $\psi(\mathbf{x}, t)$ of the quantum system being studied. A compatability with the statistical results of quantum mechanics is achieved by assigning an uncertainty in the initial conditions of the particles according to the probability density function $\rho(\mathbf{x}, 0) = |\psi(\mathbf{x}, 0)|^2$.

The causal interpretation continues to receive attention as a way of addressing the question of the incompleteness of standard quantum mechanics (see, for example, [4, 5]). Recently, however, causal trajectories have been playing a more significant role in practical calculations of chemical physics and quantum chemistry, for example (to name only a few references), quantum tunnelling dynamics [6], nonadiabatic transitions [7], reactive scattering [8], dissociation dynamics [9] and hybrid classical/quantum schemes to study complex systems [10].

Bohm himself [1] introduced the idea of studying transitions in terms of the causal interpretation, examining the Franck–Hertz experiment and the photoelectric and Compton effects. He attempted to show that the seemingly discontinuous and poorly defined transfers of energy and momentum in transitions could be accounted for in continuous matter by means

of the 'quantum potential' that arises in the causal formalism. More recently in this vein, Dewdney and Lam [11] studied transitions of (spinless) particles in a one-dimensional infinite square well potential. In this paper we employ the de Broglie–Bohm deterministic approach to study the problem of a 1s–2p electronic transition in hydrogen induced by an oscillating (semiclassical) electromagnetic field, taking the spin of the electron into account.

It is instructive to review briefly the main ideas of the causal interpretation. First, the wavefunction ψ for a particle is written in the form

$$\psi(\mathbf{x}, t) = R(\mathbf{x}, t)\, \mathrm{e}^{\mathrm{i}S(\mathbf{x},t)/\hbar} \tag{1}$$

where R and S are real valued. Substitution of equation (1) into the time-dependent Schrödinger equation,

$$\mathrm{i}\hbar \frac{\partial \psi}{\partial t} = -\frac{\hbar^2}{2m}\nabla^2\psi + V\psi \tag{2}$$

yields the following coupled equations in R and S:

$$\frac{\partial R^2}{\partial t} + \nabla \cdot \left(R^2 \frac{\nabla S}{m} \right) = 0 \tag{3}$$

and

$$\frac{\partial S}{\partial t} + \frac{(\nabla S)^2}{2m} + V + Q = 0 \tag{4}$$

where

$$Q = -\frac{\hbar^2}{2m}\frac{\nabla^2 R}{R} \tag{5}$$

is called the *quantum potential*. Equation (3) is the standard continuity equation of quantum mechanics. It can be viewed as governing the evolution of a compressible, irrotational fluid with density $\rho = \psi^*\psi = R^2$ and velocity $\mathbf{v} = \nabla S/m$ as, indeed, was done by Madelung [12]. Equation (4) has the same form as the classical Hamilton–Jacobi equation for a particle that moves under the influence of potentials V and Q. Bohm's unique interpretation of these equations was that the particle has a well-defined trajectory defined by the *quantum equation of motion*

$$\mathbf{p} = m\dot{\mathbf{x}} = \nabla S. \tag{6}$$

As stated earlier, compatability with standard quantum mechanics is achieved by viewing the initial conditions of trajectories as 'hidden variables' with associated uncertainties as described by the probability distribution $\rho(\mathbf{x}, 0)$.

Recall that the Schrödinger current $\mathbf{j}$ associated with the wavefunction ψ is given by [13]

$$\mathbf{j} = \frac{\hbar}{2m\mathrm{i}}[\psi^*\nabla\psi - \psi\nabla\psi^*]. \tag{7}$$

A comparison of equations (6) and (7) shows that

$$\mathbf{j} = \frac{1}{m}\rho\mathbf{p}. \tag{8}$$

The momentum defined in equation (6) is not unique in generating the same statistical predictions as quantum mechanics. Holland [14] has shown that equations (6) and (8) apply only to spinless particles. For particles with spin, an additional term is necessary in order that the Schrödinger equation of motion is consistent with a relativistic formulation. The condition of Lorentz invariance implies that the momentum of a particle with spin $\mathbf{s}$, even in the nonrelativistic limit, must be given by

$$\mathbf{p} = \nabla S + \nabla \log \rho \times \mathbf{s}. \tag{9}$$

The associated current

$$\mathbf{j} = \frac{1}{m}\rho\nabla S + \frac{1}{m}\nabla\rho \times \mathbf{s} \tag{10}$$

has been referred to as the *Pauli current*, the nonrelativistic limit of the *Dirac current*, as opposed to equation (8) which is the nonrelativistic limit of the *Gordon current* [15–17]. Consistency with Dirac theory requires that the Schrödinger equation be regarded as describing an electron in an eigenstate of spin [15]. As regards the causal interpretation, the spin-dependent term was also discussed in [2], but only for the Pauli equation and not the Schrödinger equation.

In the case of a hydrogen atom, the momentum equation (6) predicts that an electron in any real eigenstate will be stationary since $\nabla S = 0$. This counterintuitive result no longer applies when equation (9) is used. For example, consider an electron in the 1s ground eigenstate with wavefunction

$$\psi_{100} = \frac{1}{\sqrt{\pi a^3}}\,\mathrm{e}^{-r/a} \tag{11}$$

where $a = \hbar^2/(me^2)$ is the Bohr radius. Also assume that the electron is in a definite spin eigenstate so that its spin vector is given by $\mathbf{s} = \frac{\hbar}{2}\mathbf{k}$. Then the existence of the term $\nabla \log \rho \times \mathbf{s}$ in equation (9) implies that the electron's polar coordinates r and θ are constant and that the angle ϕ evolves in time as [3, 18]

$$\frac{\mathrm{d}\phi}{\mathrm{d}t} = \frac{\hbar}{mar}. \tag{12}$$

Therefore, the electron revolves about the z-axis at a constant angular velocity.

We also state, for future reference, the result for an electron in the (real) $2\mathrm{p}_0$ eigenstate

$$\psi_{210} = \frac{1}{\sqrt{32a^5}}r\,\mathrm{e}^{-r/2a}\cos\theta \tag{13}$$

again with spin vector $\mathbf{s} = \frac{\hbar}{2}\mathbf{k}$: The polar coordinates r and θ are again constant and the angle ϕ evolves as

$$\frac{\mathrm{d}\phi}{\mathrm{d}t} = \frac{\hbar}{2mar}. \tag{14}$$

Note that the angular velocity is one-half that of a 1s ground state electron. In [18] we examined the trajectories of electrons in a number of hydrogenic eigenstates. From equation (9), these trajectories must lie on level curves of both $|\psi|$ and z and revolve about the z-axis with constant angular velocity.

In this paper we examine solutions of the equation of motion (9) for an electron with spin vector $\mathbf{s} = \frac{\hbar}{2}\mathbf{k}$ (the 'α' or 'spin up' state) as it undergoes a transition from the 1s to $2\mathrm{p}_0$ state in hydrogen due to the presence of an oscillating electric field. We may assume that the electron has constant spin vector since the Hamiltonian describing the atom in the field (see the following section) is spin-independent. The wavefunction of the electron $\boldsymbol{\Psi}(\mathbf{x}, \mathbf{s}, t)$ may then be written as the tensor product $\psi(\mathbf{x}, t)\zeta(\mathbf{s})$ where $\zeta(\mathbf{s})$ is assumed to be an eigenfunction of the commuting spin operators $\hat{S}^2$ and $\hat{S}_z$, with $\hat{S}^2\zeta = \frac{3\hbar}{4}\zeta$ and $\hat{S}_z\zeta = \frac{\hbar}{2}\zeta$. As such, the remainder of our discussion may simply be focused on the evolution of the spatial portion of the wavefunction, $\psi(\mathbf{x}, t)$, according to equation (2).

As in the case of the examples listed above, the momentum term $\nabla \log \rho \times \mathbf{s}$ will be responsible for the revolution of the electron about the z-axis. This is accompanied by a complicated motion over a hyperboloid surface of revolution that is determined from the functional forms of the 1s and $2\mathrm{p}_0$ wavefunctions. Moreover, the course of the transition

from the ground state to the excited state can be characterized by looking at the energy of the electron along the trajectory and the angular velocity of the revolution about the z-axis. The energy and ϕ-angular velocity of the electron evolve from 1s ground state values to 2p excited state values.

In [18], as a precursor to this study, we examined the trajectories dictated by equation (9) for an electron with spin vector $\mathbf{s} = \frac{\hbar}{2}\mathbf{k}$ and spatial wavefunction that begins as a linear combination of 1s and 2p hydrogenic eigenfunctions:

$$\psi(\mathbf{x}, 0) = c_1\psi_{100}(\mathbf{x}) + c_2\psi_{210}(\mathbf{x}) \tag{15}$$

where $|c_1|^2 + |c_2|^2 = 1$. The time evolution of this wavefunction under the hydrogen atom Hamiltonian is

$$\psi(\mathbf{x}, t) = c_1\psi_{100}(\mathbf{x})\,\mathrm{e}^{-\mathrm{i}E_1t/\hbar} + c_2\psi_{210}(\mathbf{x})\,\mathrm{e}^{-\mathrm{i}E_2t/\hbar}. \tag{16}$$

Many of the qualitative features of the 1s–2p$_0$ transition problem studied below are captured by this model, most notably the invariant hyperboloid surfaces of revolution on which trajectories lie. As expected, however, the more detailed time evolution of the electron trajectories over these surfaces due to the oscillating field is missing.

2. Solution of the transition problem

The Hamiltonian used to describe this transition will have the form $\hat{H} = \hat{H}_0 + \hat{H}'$, where $\hat{H}_0$ is the hydrogen atom Hamiltonian and $\hat{H}'$ represents an oscillating electric field $\mathbf{E} = E_0 \cos \omega t\mathbf{k}$. It can be shown [19] that if ω is chosen to be sufficiently close to the 1s–2p transition frequency

$$\omega_0 = \frac{E_2 - E_1}{\hbar} \tag{17}$$

so that $\omega_0 - \omega \ll \omega_0 + \omega$, then the Hamiltonian representing the semiclassical radiation, $\hat{H}' = qzE_0 \cos \omega t$, is well approximated by

$$\hat{H}' = -\tfrac{1}{2}qzE_0\,\mathrm{e}^{-\mathrm{i}\omega t} \tag{18}$$

since the term $\mathrm{i}(\omega + \omega_0)^{-1} \sin \omega t$ is negligible. Here, q denotes the electric charge and $\omega_0 \approx 1.549 \times 10^{16}\ \mathrm{s}^{-1}$. This approach allows the equations for the wavefunction coefficients to be solved exactly so that perturbation methods need not be employed. The closeness of ω to ω_0 also allows the transition probability to approach unity at various times rather than remaining small for all times.

The probability of transition between two states $|\psi_1\rangle$ and $|\psi_2\rangle$ is related to the matrix element $\langle\psi_2|\hat{H}'|\psi_1\rangle$. In the case of the hydrogen atom the only nonvanishing matrix element is between the ground state ψ_{100} and the 2p$_0$ state ψ_{210}:

$$\begin{aligned}\langle\psi_{100}|\hat{H}'|\psi_{210}\rangle &= -\langle\psi_{100}|qE_0r\cos\theta|\psi_{210}\rangle\tfrac{1}{2}\,\mathrm{e}^{-\mathrm{i}\omega t} \\ &= -\frac{64\sqrt{2}}{243}aqE_0\,\mathrm{e}^{-\mathrm{i}\omega t}.\end{aligned} \tag{19}$$

The time-dependent wavefunction can be written as a linear combination of $|\psi_{100}\rangle$ and $|\psi_{210}\rangle$:

$$\psi(t) = c_a(t)\psi_{100}\,\mathrm{e}^{-\mathrm{i}E_1t/\hbar} + c_b(t)\psi_{210}\,\mathrm{e}^{-\mathrm{i}E_2t/\hbar}. \tag{20}$$

Substitution into the Schrödinger equation yields the following equations for $c_a(t)$ and $c_b(t)$:

$$\dot{c}_a = -\frac{\mathrm{i}}{\hbar}\frac{V_{12}}{2}\,\mathrm{e}^{-\mathrm{i}(\omega_0-\omega)t}c_b \qquad \dot{c}_b = -\frac{\mathrm{i}}{\hbar}\frac{V_{12}}{2}\,\mathrm{e}^{\mathrm{i}(\omega_0-\omega)t}c_a \tag{21}$$

where

$$V_{12} = -\frac{128\sqrt{2}}{243}aqE_0.$$

These DEs can be solved exactly to give

$$\begin{aligned} c_a(t) &= \frac{\sigma+\Omega}{2\sigma}\,\mathrm{e}^{\frac{1}{2}\mathrm{i}(\Omega-\sigma)t} + \frac{\sigma-\Omega}{2\sigma}\,\mathrm{e}^{\frac{1}{2}\mathrm{i}(\Omega+\sigma)t} \\ c_b(t) &= \frac{\nu}{2\sigma}\,\mathrm{e}^{\frac{1}{2}\mathrm{i}(\Omega-\sigma)t} - \frac{\nu}{2\sigma}\,\mathrm{e}^{\frac{1}{2}\mathrm{i}(\Omega+\sigma)t} \end{aligned} \tag{22}$$

where

$$\Omega = \omega_0 - \omega \qquad \nu = \frac{V_{12}}{\hbar} \qquad \sigma = \sqrt{\Omega^2+\nu^2}. \tag{23}$$

The wavefunction $\psi(\mathbf{x}, t)$ may now be written explicitly as

$$\psi(\mathbf{x}, t) = \frac{1}{\sqrt{\pi a^3}} c_a(t)\,\mathrm{e}^{-r/a}\,\mathrm{e}^{-\mathrm{i}E_1 t/\hbar} + \frac{1}{\sqrt{32\pi a^5}} c_b(t) r\,\mathrm{e}^{-r/2a}\cos\theta\,\mathrm{e}^{-\mathrm{i}E_2 t/\hbar}. \tag{24}$$

To compute the momentum according to equation (9), note that the wavefunction, and hence the first term ∇S, has only $\hat{r}$ and $\hat{\theta}$ components. Since we are assuming a constant spin vector $\mathbf{s} = \frac{\hbar}{2}\hat{k}$, it follows that the vector $\nabla \log\rho \times \mathbf{s}$ points in the $\hat{\phi}$ direction.

Calculating ∇S from equation (24) yields

$$p_{\hat{r}} = \frac{\hbar\nu\beta}{2\sigma}\frac{\cos\theta\,\mathrm{e}^{-3r/2a}\left(1+\frac{r}{2a}\right)T(t)}{D(r,\theta,t)} \qquad p_{\hat{\theta}} = -\frac{\hbar\nu\beta}{2\sigma}\frac{\sin\theta\,\mathrm{e}^{-3r/2a}T(t)}{D(r,\theta,t)} \tag{25}$$

where $\beta = 4\sqrt{2}a$ is the ratio of the normalizing factors of the two wavefunctions,

$$T(t) = -\cos\omega_0 t\,\sin\sigma t - \frac{\Omega}{\sigma}\sin\omega_0 t + \frac{\Omega}{\sigma}\cos\sigma t\,\sin\omega_0 t \tag{26}$$

and

$$\begin{aligned} D(r,\theta,t) = {} & \mathrm{e}^{-2r/a}\frac{1}{2\sigma^2}(\sigma^2+\Omega^2+\nu^2\cos\sigma t) + \beta^2 r^2\,\mathrm{e}^{-r/a}\cos^2\theta\,\frac{\nu^2}{2\sigma^2}(1-\cos\sigma t) \\ & + \frac{\nu}{\sigma}\beta r\,\mathrm{e}^{-\frac{3r}{2a}}\cos\theta\left(\frac{\Omega}{\sigma}\cos\omega_0 t - \frac{\Omega}{\sigma}\cos\sigma t\cos\omega_0 t - \sin\omega_0 t\sin\sigma t\right). \end{aligned} \tag{27}$$

The denominator $D(r, \theta, t)$ in the above expressions is proportional to $|\psi(\mathbf{x}, t)|^2$.

The second term in equation (9), $\nabla \log\rho \times \mathbf{s}$, can be computed in the (right-handed) spherical polar coordinate system

$$\mathbf{A}\times\mathbf{B} = \begin{vmatrix} \hat{\theta} & \hat{\phi} & \hat{r} \\ A_\theta & A_\phi & A_r \\ B_\theta & B_\phi & B_r \end{vmatrix}. \tag{28}$$

Using the simplification

$$\nabla\log\rho = 2\,\mathrm{Re}\left(\frac{(\nabla\psi)\psi^*}{\psi^*\psi}\right)$$

we find the $\hat{\phi}$ component of the momentum to be

$$p_{\hat{\phi}} = \frac{\hbar\beta}{D}(-\chi_r\sin\theta - \chi_\theta\cos\theta) \tag{29}$$

where

$$\begin{aligned} \chi_r &= \frac{1}{\beta a}|c_a|^2\,\mathrm{e}^{-2r/a} + \beta|c_b|^2\cos^2\theta\,\mathrm{e}^{-r/a} r\left(1-\frac{r}{2a}\right) + \cos\theta\,\mathrm{e}^{-3r/2a}\left(1-\frac{3r}{2a}\right)T'(t) \\ \chi_\theta &= -\beta|c_b|^2\,\mathrm{e}^{-r/a}\sin\theta\cos\theta r - \mathrm{e}^{-3r/2a}\sin\theta T'(t) \end{aligned}$$

and

$$T'(t) = \frac{\nu}{2\sigma}\left(\frac{\Omega}{\sigma}\cos\omega_0 t - \frac{\Omega}{\sigma}\cos\sigma t\cos\omega_0 t - \sin\sigma t\sin\omega_0 t\right). \tag{30}$$

In summary, the three components of the momentum are given by equations (25) and (29). It is worth noting that the spin-dependent momentum term $\nabla\log\rho\times\mathbf{s}$ in equation (9) is responsible for the ϕ-momentum $p_{\hat{\phi}}$.

It is useful to rescale these equations by defining the following dimensionless variables:

$$\xi = \frac{r}{a} \qquad \tau = \omega_0 t. \tag{31}$$

In these variables, equations (25) and (29) give rise to the following system of differential equations in ξ, θ and ϕ as functions of τ:

$$\begin{aligned}
\frac{\mathrm{d}\xi}{\mathrm{d}\tau} &= \frac{\nu}{3\sqrt{2}\sigma}\left(\cos\theta\,\mathrm{e}^{-3\xi/2}\left(1+\frac{\xi}{2}\right)\right)\frac{\tilde{T}(\tau)}{D}\\
\frac{\mathrm{d}\theta}{\mathrm{d}\tau} &= -\frac{\nu}{3\sqrt{2}\sigma}\left(\sin\theta\frac{\mathrm{e}^{-3\xi/2}}{\xi}\right)\frac{\tilde{T}(\tau)}{D}\\
\frac{\mathrm{d}\phi}{\mathrm{d}\tau} &= \frac{\nu}{3\sqrt{2}\sigma\xi D}(\chi_r+\chi_\theta\cot\theta)
\end{aligned} \tag{32}$$

where $\tilde{T}(\tau) = T(t)$ and we have used the following relations:

$$\frac{\mathrm{d}\phi}{\mathrm{d}\tau} = \frac{p_\phi}{ma\omega_0\xi\sin\theta}$$

and

$$\frac{\hbar}{ma\omega_0} = \frac{8}{3}a.$$

Some important qualitative features of the solutions to these DEs may be extracted. First note that the ξ and θ DEs are independent of ϕ. From these two equations, we have

$$\frac{\mathrm{d}\xi}{\mathrm{d}\theta} = -\xi\left(1+\frac{\xi}{2}\right)\cot\theta. \tag{33}$$

This DE is easily solved to give [18]

$$\xi = \frac{2}{A\sin\theta - 1} \qquad A = \frac{2+\xi_0}{\xi_0\sin\theta_0} > 1 \tag{34}$$

where $\xi_0 = \xi(0)$ and $\theta_0 = \theta(0)$. This relation defines a family of hyperbolas in vertical planes that contain the z-axis, i.e. $\phi = \phi_0$, a constant. (Note that the right-hand side of equation (33) is determined by the functional forms of the 1s and $2p_0$ wavefunctions. Other allowable pairs of wavefunctions will yield different types of curves.) The solutions of equation (32) therefore lie on surfaces that are obtained by rotating these hyperbolas about the z-axis (see [18] for a more detailed discussion). However, the time-dependent behaviour of the trajectories lying on these invariant sets must be determined numerically.

3. Numerical results

In choosing the parameters for the numerical integration, there are various factors that must be taken into account. First, recall that in order to use the Hamiltonian $\hat{H}' = -\frac{1}{2}qzE_0\,\mathrm{e}^{-\mathrm{i}\omega t}$, we require that the perturbing frequency ω be close to the transition frequency ω_0 so that $\Omega = \omega_0 - \omega \ll \omega_0 + \omega$. Therefore, we cannot allow Ω to be too large, i.e. $\Omega \leqslant O(10^{13})$.

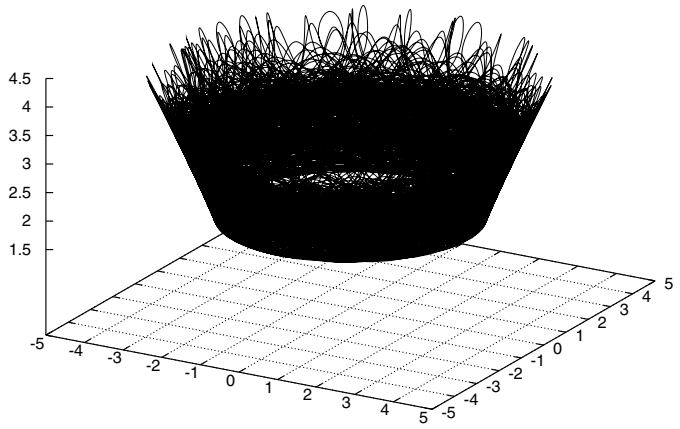

Figure 1. Trajectory of electron in $\mathbf{R}^3$ during 1s–2p$_0$ transition: $\xi(0) = 4, \theta(0) = 1$.

If we wish to be fairly confident that a transition will occur, it is also necessary that the coefficient c_b becomes large in magnitude at some time, i.e. roughly unity. Recall from equation (22) that $c_b \propto \nu/2\sigma$, and $\nu \propto E_0$. Also, the derivatives in equation (32) are proportional to $\nu/2\sigma$, and it is desirable for numerical integration that they evaluate to order 1. Therefore, $|\nu|$ should be significant compared to 2σ. Now, recall that $\sigma = \sqrt{\Omega^2 + \nu^2}$ so that

$$\frac{|\nu|}{2\sigma} = \frac{1}{2}\left[\frac{\Omega^2}{\nu^2} + 1\right]^{-1/2}.$$

Therefore, we require that $|\nu|$ is not too large. Because $|\nu|$ is proportional to the field strength, we are free to choose a small value.

Another factor to consider is that there are two angular frequencies in the problem, namely σ and ω_0 from equations (26) and (30). For numerical stability it is best if these are within several orders of magnitude of each other. Therefore, σ should not be too small in comparison with ω_0. It is also desirable that c_b becomes significant in a reasonable time. From equation (22), we find that

$$|c_b(t)|^2 = \left(\frac{\nu}{\sigma}\right)^2 \sin^2 \frac{\sigma}{2} t. \tag{35}$$

Therefore, having σ appropriately scaled will mean that there is a high probability of seeing a transition within a reasonable time.

The above considerations imply that:

1. $|\nu|$ cannot be too large because $[\Omega^2/\nu^2 + 1]^{-1/2}$ must be O(1),
2. $\sigma = \sqrt{\Omega^2 + \nu^2}$ cannot be more than several orders of magnitude smaller than ω_0 and
3. we cannot increase σ by increasing Ω, because we require that $\Omega \leqslant O(10^{13})$.

With these points in mind, the parameters have been chosen as follows:

$$E_0 = 8.8 \times 10^7 \text{ V m}^{-1} \qquad \Omega = 1.55 \times 10^{12} \text{ s}^{-1} \tag{36}$$

so that

$$\nu = -5.1 \times 10^{12} \qquad \sigma = 5.32 \times 10^{12}. \tag{37}$$

The results of numerical integration for two choices of initial conditions are shown in figures 1 and 2. Figures 3 and 4 show the same trajectories split over five consecutive time

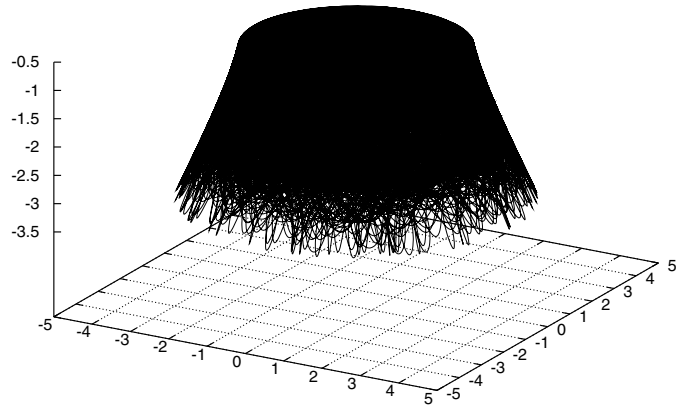

Figure 2. Trajectory of electron in $\mathbf{R}^3$ during 1s–2p$_0$ transition: $\xi(0) = 3.2$, $\theta(0) = 2$.

intervals. In these latter plots, the hyperboloid surfaces of revolution on which the trajectories lie, described at the end of the previous section, are discernable.

In standard semiclassical treatments of this problem (see, for example, [13], pp 282–5), the maximum probability of transition occurs when $\sin^2 \frac{1}{2}\Omega t = 1$, or $\Omega t = (2k + 1)\pi$ for $k = 0, 1, 2, \ldots$. In our formulation, from equation (35) the maximum probability of transition occurs when $\sin^2 \frac{1}{2}\sigma t = 1$, or $\sigma t = (2k + 1)\pi$ for $k = 0, 1, 2, \ldots$. In other words, the dependence on Ω is replaced with one on $\sigma = \sqrt{\Omega^2 + \nu^2}$. This is due to our choice of Hamiltonian and the fact that the equations in (22) result from an exact integration of equation (21) rather than a perturbation approach. From above, the first occurrence of the maximum probability of transition in our problem will occur at $t = \pi/\sigma$ or, in dimensionless time, $\tau = \pi\omega_0/\sigma$. From the numerical values chosen for the parameters above, this corresponds to $\tau \approx 9000$.

The causal interpretation allows us to examine the process in more detail by looking at the angular velocity $\dot{\phi}$ exhibited by the trajectories. At time $t = \tau = 0$, each trajectory begins at the 1s ground state wavefunction, namely, $c_a(0) = 1$ and $c_b(0) = 0$, and we expect the electron to revolve about the z-axis with angular frequency given by equation (12). When the wavefunction is approximately equal to the 2p$_0$ eigenstate, namely, $c_a \approx 0$ and $c_b \approx 1$, then we expect $\dot{\phi}$ to be given roughly by equation (14).

Since the computations were performed in scaled variables ξ and τ, cf equation (31), we must first rescale the 1s and 2p$_0$ angular velocities in ϕ, cf equations (12) and (14), in order to assess the numerical results. For the 1s state, equation (12) becomes

$$\frac{\mathrm{d}\phi}{\mathrm{d}\tau} = \frac{\hbar}{ma^2\omega_0\xi} = \frac{8}{3\xi}. \tag{38}$$

The angular velocity for the 2p$_0$ state is simply one-half of the above result.

The values of the scaled angular velocity $\mathrm{d}\phi/\mathrm{d}\tau$ associated with the trajectory shown in figure 1 are presented as a function of τ in figure 5. (Figure 6 shows the corresponding values of ϕ.) Recall that this trajectory began with the value $\xi(0) = 4$. From figure 1, $\mathrm{d}\phi/\mathrm{d}\tau$ is observed to be roughly $2/3$ near $\tau = 0$. This is in agreement with equation (38)—the electron is revolving about the z-axis at the 1s rate.

Near $\tau = 9000$, roughly the time for $|c_b(\tau)^2|$ to achieve its maximum value, we observe that $\mathrm{d}\phi/\mathrm{d}\tau \approx 0.3$. At that time, $\xi \approx 4.5$. This is in agreement with the scaled 2p$_0$ rate $4/(3\xi) \approx 0.3$.

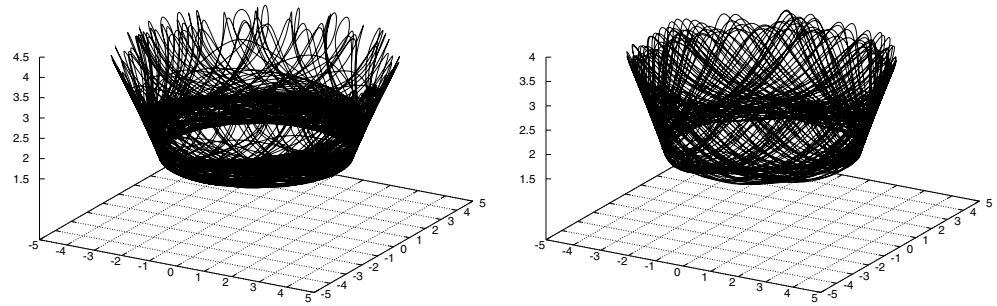

(a) $\tau = 0{-}1469$

(b) $\tau = 1469{-}2992$

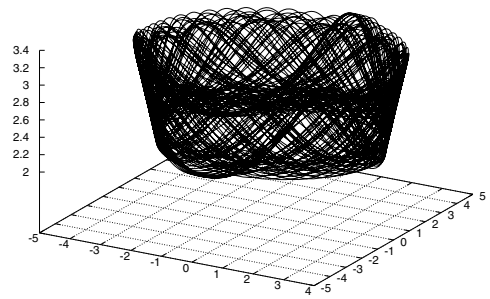

(c) $\tau = 2992{-}4844$

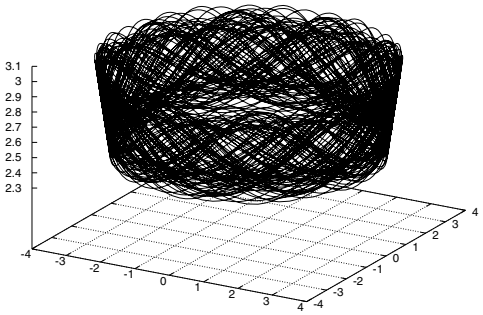

(d) $\tau = 4844{-}7196$

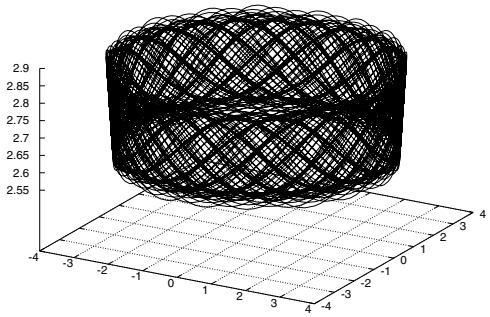

(e) $\tau = 7196{-}10000$

Figure 3. Trajectory of electron in $\mathbf{R}^3$ during 1s–2p$_0$ transition, split over five time intervals: $\xi(0) = 4, \theta(0) = 1$.

In the causal interpretation it is also possible to ascribe a value of energy along a trajectory and thereby examine the time-dependent behaviour of the energy during a transition. Note that this is in contrast to standard quantum mechanics, in which we can only compute probabilities of measuring energy eigenstates E_1 or E_2 after the perturbation has been turned off. One method of computing the energy is to use the result $E = -\partial S/\partial t$ implied by the Hamilton–Jacobi equation (4). However, even when applied to the relatively simple wavefunction ψ in equation (24), this method is quite cumbersome. On the other hand, Holland's method of assigning values of an observable quantity A to points on a trajectory, which we outline below (see [3], pp 91–3), is quite easily implemented in our problem.

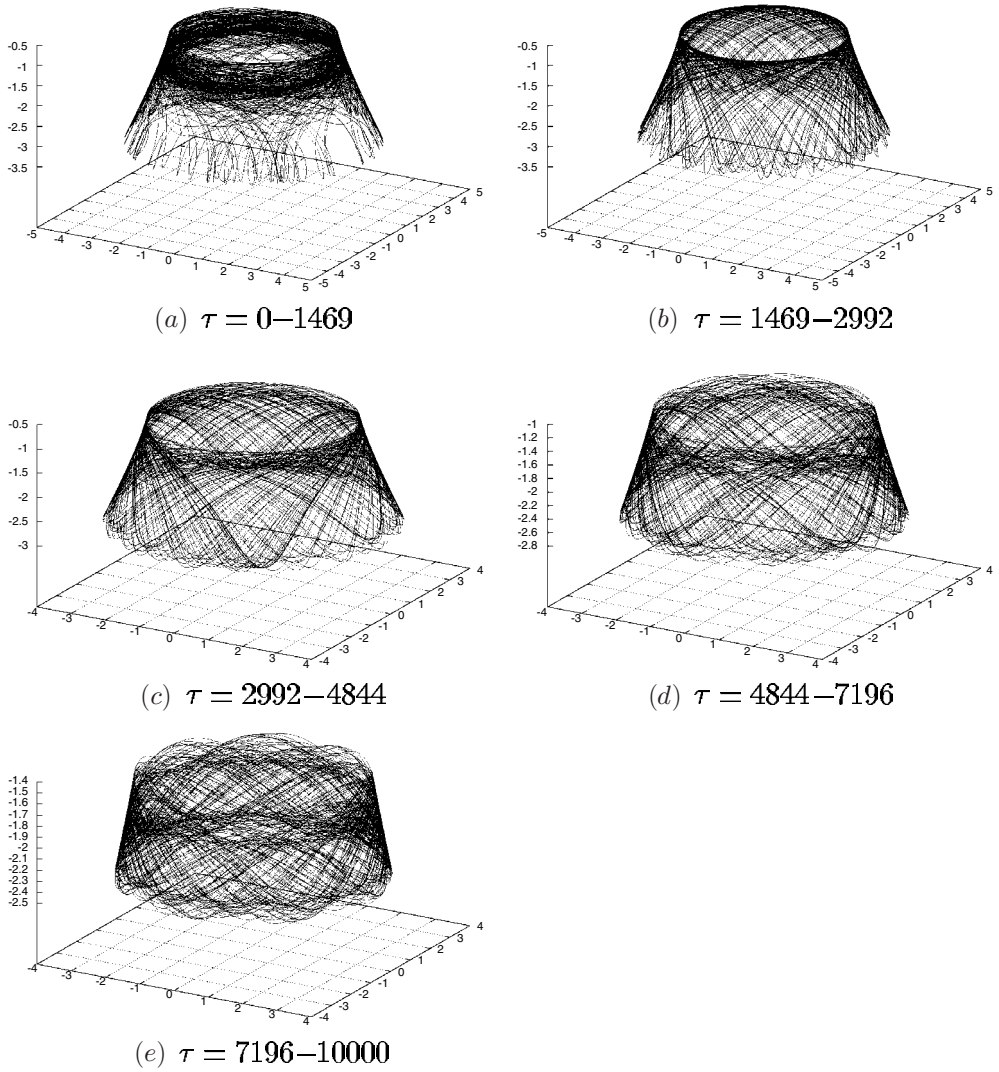

(*a*) $\tau = 0$–1469 (*b*) $\tau = 1469$–2992

(*c*) $\tau = 2992$–4844 (*d*) $\tau = 4844$–7196

(*e*) $\tau = 7196$–10000

Figure 4. Trajectory of electron in $\mathbf{R}^3$ during 1s–2p$_0$ trajectory, split over five time intervals: $\xi(0) = 3.2, \theta(0) = 2$.

The usual expectation value of an observable $\hat{A}$ is

$$\langle \hat{A} \rangle = \langle \psi | \hat{A} | \psi \rangle = \frac{\int \psi^* \hat{A} \psi \, \mathrm{d}^3\mathbf{x}}{\int \psi^* \psi \, \mathrm{d}^3\mathbf{x}}.$$

Since $\hat{A}$ must be Hermitian, ultimately only the real portion of the expression contributes to the integral. Hence define the *local* expectation value to be

$$A(\mathbf{x}, t) = \frac{\mathrm{Re}\{\psi^* \hat{A} \psi\}}{\psi^* \psi}. \tag{39}$$

To find the local energy expectation value along the trajectory, we compute this quantity using the Hamiltonian $\hat{H} = \hat{H}_0 + \hat{H}'$ where, as before, $\hat{H}_0$ is the usual hydrogen Hamiltonian, and

$$\hat{H}' = -\tfrac{1}{2} e E_0 \, \mathrm{e}^{-\mathrm{i}\omega t} (r \cos\theta).$$

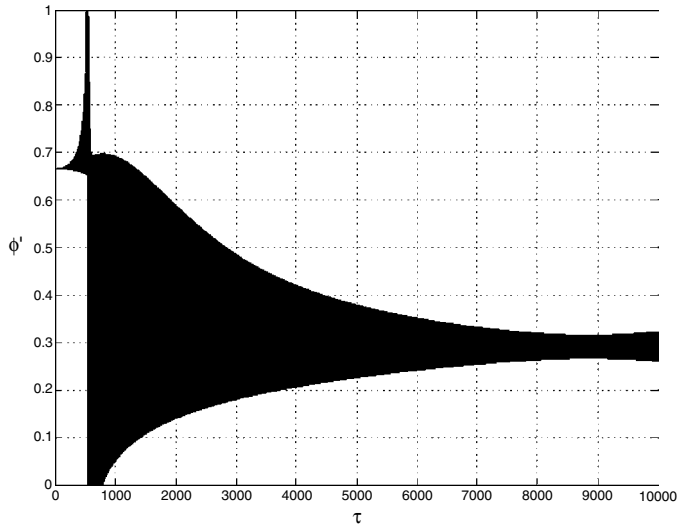

Figure 5. Scaled angular velocity $\frac{d\phi}{d\tau}$ along the trajectory shown in figure 1.

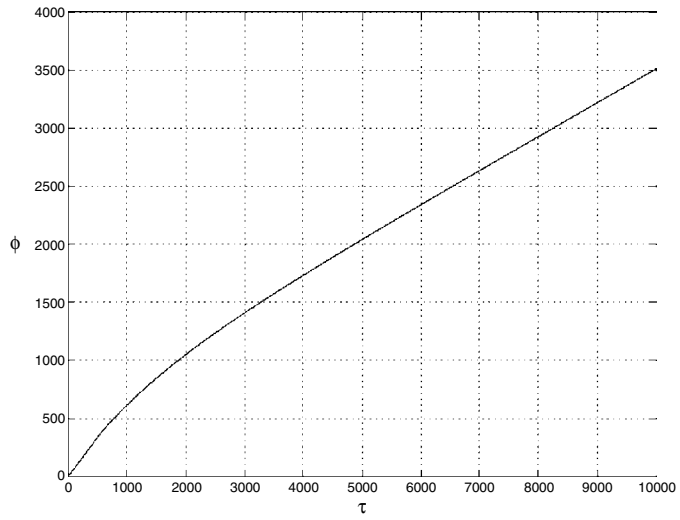

Figure 6. Angle $\phi(\tau)$ along the trajectory shown in figure 1.

Thus

$$E(\mathbf{x}, t) = \frac{\mathrm{Re}\{\psi^*(\hat{H}_0 + \hat{H}')\psi\}}{\psi^*\psi} = \frac{\mathrm{Re}\{\psi^*\hat{H}_0\psi\}}{\psi^*\psi} + \frac{\mathrm{Re}\{\psi^*\hat{H}'\psi\}}{\psi^*\psi} \tag{40}$$

where $\psi(\mathbf{x}, t)$ is given by equation (20). Note that the relationship to the classical energy is not direct; this local energy expectation value is not a first integral of motion, simply a quantity whose average, over trajectories, yields the quantum mechanical energy expectation

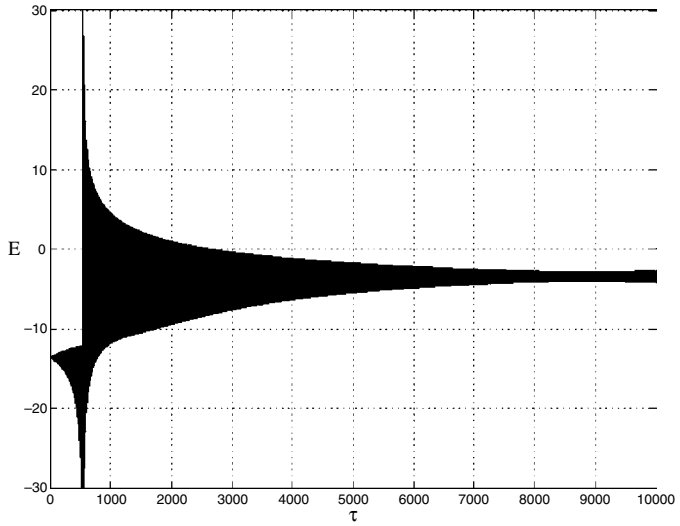

Figure 7. Energy (eV) along the trajectory in figure 1.

value. Here we will refer to it as the local energy. After some manipulations, the first term in equation (40) is given by

$$\frac{\mathrm{Re}\{\psi^*(\hat{H}_0)\psi\}}{\psi^*\psi} = \frac{|c_a|^2 E_1 \psi_{100}^2 + |c_b|^2 E_2 \psi_{210}^2 + \psi_{100}\psi_{210}(E_2+E_1)\mathrm{Re}\{c_a c_b\, \mathrm{e}^{-\mathrm{i}\omega t}\}}{\psi^*\psi}$$

and the second term is simply

$$\frac{\mathrm{Re}\{\psi^* \hat{H}'\psi\}}{\psi^*\psi} = \frac{\mathrm{Re}\left\{\psi^*\left(-\tfrac{1}{2}\, eE_0\, \mathrm{e}^{-\mathrm{i}\omega t}(r\cos\theta)\psi\right)\right\}}{\psi^*\psi} = -\frac{1}{2}\, eE_0 r\cos\theta\cos\omega t$$

where, referring to equation (30),

$$\mathrm{Re}\{c_a c_b\, \mathrm{e}^{-\mathrm{i}\omega t}\} = \frac{\nu}{2\sigma}\left(\frac{\Omega}{\sigma}\cos\omega_0 t - \frac{\Omega}{\sigma}\cos\sigma t\cos\omega_0 t - \sin\sigma t\sin\omega_0 t\right) = T'(t).$$

Therefore we have

$$E = \frac{|c_a|^2 E_1 \psi_{100}^2 + |c_b|^2 E_2 \psi_{210}^2 + \psi_{100}\psi_{210}(E_2+E_1)T'(t)}{\psi^*\psi} - \frac{1}{2}\, eE_0 r\cos\theta\cos\omega t. \tag{41}$$

This function can be evaluated along the trajectories shown in figures 1 and 2. The results for the first trajectory are shown in figure 7.

Note that at $\tau = 0$, the local energy is equal to the 1s ground state energy -13.6 eV, and that after the transition, the energy oscillates near the value of $E_2 = -3.4$ eV, corresponding to the energy of hydrogenic $n = 2$ states. The energy is not constant even in the proximity of these points because of the extra oscillating perturbation $\hat{H}'$ that represents the semiclassical radiation field. The spike in the energy corresponds to a point along the trajectory that approaches a zero of the wavefunction. Intuitively, one can understand the appearance of such a spike because the electron cannot spend time in regions where $\psi^*\psi$ is very small—it receives a 'kick' from the quantum potential which corresponds to a sudden rise in its energy.

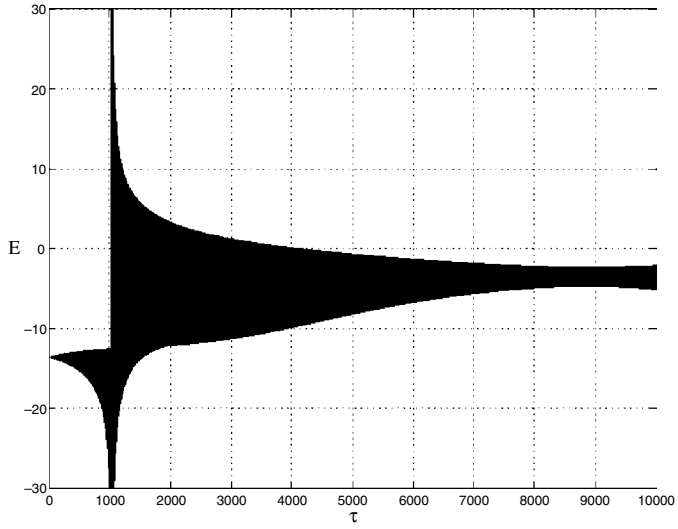

Figure 8. Energy (eV) along the trajectory in figure 2.

Plots of the quantum potential for several systems and a discussion are given in Holland [3] and references within, for example, [20, 21]. The energy along the trajectory shown in figure 2 is shown in figure 8.

Finally, we mention that we have computed trajectories to higher times. At $\tau \approx 18\,000$, the scaled angular velocity $\mathrm{d}\phi/\mathrm{d}\tau$ is observed to oscillate about the 1s value. The energy is also observed to oscillate about the 1s value of -13.6 eV. This is in accordance with $|c_b(\tau)|^2 \approx 0$ from equation (35) and the values of the parameters used in the calculation. We conclude that the transition has reversed and that the electron has returned to the 1s ground state.

4. Concluding remarks

We have studied the problem of a simple 1s to $2p_0$ electronic transition in hydrogen—induced by an oscillating (semiclassical) radiation field—in terms of the causal interpretation of quantum mechanics. In contrast to Bohm's original formulation $\mathbf{p} = \nabla S$, however, we have employed an additional spin-dependent term $\nabla \log \rho \times \mathbf{s}$ in the equation of motion, where $\rho = \psi^*\psi$. The electron is assumed to be in a 'spin up' eigenstate, with associated spin vector $\mathbf{s} = \frac{\hbar}{2}\mathbf{k}$, during the transition. The electronic trajectories lie on invariant hyperboloid surfaces of revolution about the z-axis. The nature of the trajectories over these surfaces is quite complex due to the quasi-periodic nature of the equations of motion which, in turn, arise from the interplay of the 1s–2p transition frequency ω_0, the frequency ω of the oscillating radiation and E_0, the field strength.

As the electron moves over the invariant surface it also revolves about the z-axis due to the spin-dependent momentum term. The progress of the transition can be tracked by observing the local energy E and the angular velocity $\dot{\phi}$ of the electron. Beginning at values associated with the 1s ground state, both quantities are seen to evolve towards values associated with the $2p_0$ excited state in time. The causal interpretation has offered a way to examine the phenomenon of transition which is not limited to computing the probabilities of measuring E_1 and E_2 at various times after the perturbation has been turned off.

Acknowledgments

We gratefully acknowledge that this research has been supported by the Natural Sciences and Engineering Research Council of Canada (NSERC) in the form of a Postgraduate Scholarship (CC) and an Individual Research Grant (ERV). CC also acknowledges partial financial support from the Province of Ontario (Graduate Scholarship) as well as the Faculty of Mathematics, University of Waterloo.

References

[1] Bohm D 1952 A suggested interpretation of the quantum theory in terms of 'hidden' variables I/II *Phys. Rev.* A **85** 166/180
[2] Bohm D and Hiley B J 1993 *The Undivided Universe: an Ontological Interpretation of Quantum Theory* (London: Routledge)
[3] Holland P 1993 *The Quantum Theory of Motion: an Account of the de Broglie–Bohm Causal Interpretation of Quantum Mechanics* (Cambridge: Cambridge University Press)
[4] Afriat A and Selleri F 1999 *The Einstein, Podolsky and Rosen Paradox in Atomic, Nuclear and Particle Physics* (New York: Plenum)
[5] Cushing J T, Fine A and Goldstein S 1996 *Bohmian Mechanics and Quantum Theory: an Appraisal* (Dordrecht: Kluwer Academic)
[6] Bittner E 2000 Quantum tunneling dynamics using hydrodynamic trajectories *J. Chem. Phys.* **112** 9703–10
[7] Burant J C and Tully J C 2000 Nonadiabatic dynamics via the classical limit Schrödinger equation *J. Chem. Phys.* **112** 6097–103
[8] Wyatt R E 1999 Quantum wave packet dynamics with trajectories: application to reactive scattering *J. Chem. Phys.* **111** 4406–13
[9] Wang Z S, Darling G R and Holloway S 2001 Dissociation dynamics from a de Broglie–Bohm perspective *J. Chem. Phys.* **115** 10373–81
[10] Gindensperger E, Meier C and Beswick J A 2000 Mixing quantum and classical dynamics using Bohmian trajectories *J. Chem. Phys.* **113** 9369–72
[11] Dewdney C and Lam M M 1991 What happens during a quantum transition? *Information Dynamics* ed H Atmanspacher and H Scheingraber (New York: Plenum)
[12] Madelung E 1926 Quantentheorie in hydrodynamischer Form *Z. Phys.* **40** 322–6
[13] Schiff L 1955 *Quantum Mechanics* (New York: McGraw-Hill)
[14] Holland P 1999 Uniqueness of paths in quantum mechanics *Phys. Rev.* A **60** 4326
[15] Gurtler R and Hestenes D 1975 Consistency in the formulation of the Dirac, Pauli and Schrödinger theories *J. Math. Phys.* **16** 573
[16] Hestenes D 1975 Observables, operators and complex numbers in the Dirac theory *J. Math. Phys.* **16** 556
[17] Hestenes D 1979 Spin and uncertainty in the interpretation of quantum mechanics *Am. J. Phys.* **47** 399
[18] Colijn C and Vrscay E R 2002 Spin-dependent Bohm trajectories for hydrogen eigenstates *Phys. Lett.* A **300** 334
[19] Griffiths D 1995 *Introduction to Quantum Mechanics* (Englewood Cliffs, NJ: Prentice-Hall)
[20] Dewdney C and Hiley B J 1982 A quantum potential description of one-dimensional time-dependent scattering from square barriers and square wells *Found. Phys.* **12** 27–48
[21] Philippidis C, Dewdney C and Hiley B J 1979 *Nuovo Cimento* B **52** 15